Inorganic Chemistry

Article

pubs.acs.org/IC

Use of a Bidentate Ligand Featuring an *N*-Heterocyclic Phosphenium Cation (NHP$^+$) to Systematically Explore the Bonding of NHP$^+$ Ligands with Nickel

Mark W. Bezpalko, Bruce M. Foxman, and Christine M. Thomas*

Department of Chemistry, Brandeis University, 415 South Street MS 015, Waltham, Massachusetts 02454, United States

Supporting Information

ABSTRACT: A novel bidentate ligand featuring an *N*-heterocyclic phosphenium cation (NHP$^+$) linked to a phosphine side arm is used to explore the coordination chemistry of NHP$^+$ ligands with nickel. Direct P−Cl bond cleavage from a chlorophosphine precursor [PP]-Cl (**1**) by Ni(COD)$_2$ affords the asymmetric bimetallic complex [Cl$_2$Ni(μ-PP)$_2$Ni] (**2**) via a nonoxidative process. Abstraction of the halide with either NaBPh$_4$ or K[B(C$_6$F$_5$)$_4$] prior to metal coordination to form the free phosphenium ligand [PP]$^+$ *in situ*, followed by coordination to Ni(COD)$_2$, afforded the halide-free Ni^0 complexes [(PP)Ni(COD)] [B(C$_6$F$_5$)$_4$] (**4**) and [(PP)Ni(COD)][BPh$_4$] (**5**). Chloride abstraction from **1** is problematic in the presence of a PF$_6^-$ counterion, however, as evident by the formation of [(PP)Ni(PP-F)][PF$_6$] (**3**). The COD ligand in **5** can be readily displaced with PMe$_3$ or PPh$_3$ to afford [(PP)NiL$_2$][BPh$_4$] (L = PMe$_3$ (**6**), PPh$_3$ (**7**)). Complexes **2**−**7** feature planar geometries about the NHP$^+$ phosphorus atom and unusually short Ni−P distances, indicative of multiple bonding resulting from both P → Ni σ donation and Ni → P π backbonding. This bonding description is supported by theoretical studies using natural bond orbital analysis.

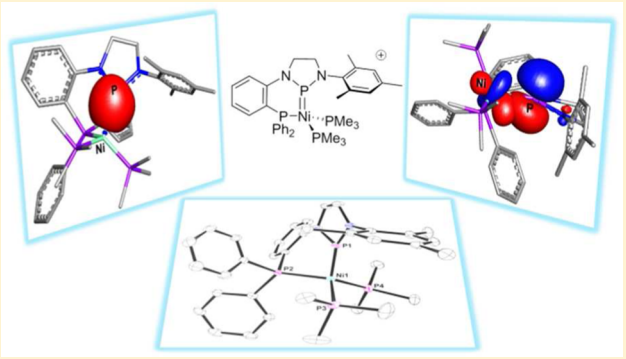

INTRODUCTION

N-heterocyclic phosphenium cations (NHP$^+$'s) are strongly electrophilic ligands that are largely unexplored in transition metal coordination chemistry, particularly in comparison to N-heterocyclic carbenes.[1] The vast majority of NHP coordination chemistry has been reported with second and third row transition metals, including both monometallic and bimetallic Pd, Pt, and Rh species.[2] The examples of first row transition metal complexes of NHP$^+$ ligands are largely dominated by Fe and Co carbonyl complexes.[3] To date, the only reported examples of a Ni NHP$^+$ complex are the [(^{Me}NHP)Ni(CO)$_3$]$^+$ cation, (where the "R" in ^{R}NHP represents the substituents on nitrogen), which was reported without structural characterization in 1987,[4] and several Ni NHP$^+$ complexes described in conference proceedings by Baker and co-workers that remain unpublished.[5]

Owing to their cationic nature, NHP$^+$'s are weak σ-donor ligands but strong π-acceptors, bringing to mind analogies to carbonyl ligands. Our group and others have shown that, in addition to the expected planar binding mode, NHP$^+$ cations can also adopt a pyramidal geometry when binding to transition metals.[2b,3a,d] One can explain this sort of pyramidal geometry using two possible descriptions, either (1) the phosphenium cation acts exclusively as an acceptor, with a nonbonding phosphorus lone pair or (2) the NHP ligand can be thought of as an NHP$^-$ phosphido ligand that has formally oxidized the metal center by two electrons. Formalisms aside, the ability to adopt two different binding modes in response to electronic changes at the transition metal to which they are bound provides a compelling analogy between phosphenium cations and nitrosyls.[2d,6] The obvious advantage of NHP$^+$ ligands over their diatomic carbonyl and nitrosyl analogues is the ability to readily tune their steric and electronic properties and/or incorporate NHP$^+$ cations into chelating frameworks to promote metal coordination.

Recently, our group reported the first example of a chelating ligand that incorporates an NHP$^+$ cation, namely a pincer ligand with a central NHP$^+$ unit and two phosphine side arms appended by aryl linkers, [PPP]$^+$ (Chart 1).[7] Upon coordination to d^{10} metal ions including Co^{-I}, Pd^0, and Pt^0, we have found that the NHP/diphosphine ligand shows a strong preference to adopt a pyramidal geometry at the central NHP phosphorus atom.[2b,3a] In addition to computational analyses that suggest covalent M−P bonds suggestive of metal-phosphidos, the square planar geometry of the four-coordinate {[PPP]M-L/X}$^{+/0}$ complexes (M = Pd, Pt) provides particularly compelling evidence that these compounds are best described as NHP$^-$/M^{II} complexes.[2b] Structural and computational studies have also shown that the pyramidal NHP$^-$ and planar NHP$^+$ geometries can interconvert upon electronic changes at the bound transition metal, including the

Received: June 17, 2015
Published: August 24, 2015

DOI: 10.1021/acs.inorgchem.5b01363
Inorg. Chem. 2015, 54, 8717−8726

Chart 1. Molecular Structures of Analogous Compounds Supported by a Monodentate NHP$^+$ Ligand and a Chelating NHP/Diphosphine Pincer Ligand[2b,e]

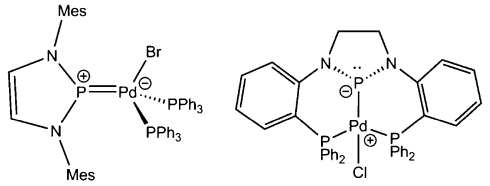

addition/removal of ancillary ligands or two-electron redox changes.[2b]

An interesting question thus arises as to how the incorporation of the NHP unit into a chelating pincer framework impacts the transition metal binding modes. The difference is particularly striking when one compares Pt and Pd complexes with identical coordination numbers and ligand types such as the tetrahedral complex (u^{Mes}NHP)Pd(Br)-$(PPh_3)_2$ and [PPP]PdX (Chart 1, where "u" represents an unsaturated heterocycle and Mes = 2,4,6-trimethylphenyl).[2b,e] We hypothesized that the rigid geometry of the pincer ligand upon coordination was responsible. *N*-aryl substituted NHP$^+$ (and NHC) ligands typically adopt geometries in which the *N*-aryl substituents are oriented nearly perpendicular to the *N*-heterocyclic ring, but the *N*-aryl rings of the [PPP]$^+$ pincer ligand are forced to be approximately coplanar with the heterocycle in the case of the pincer ligand. We posited that this coplanarity permitted delocalization of the nitrogen lone pairs throughout the aromatic rings, diminishing π-donation to phosphorus and stabilizing the anionic *N*-heterocyclic phosphido fragment (Figure 1). To test this hypothesis, we have now synthesized a bidentate NHP$^+$/phosphine ligand featuring just one aryl-linked phosphine side arm.

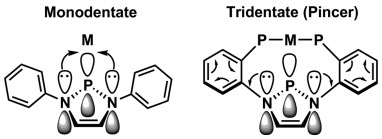

Figure 1. Hypothesized mechanism by which aromatic delocalization stabilizes an NHP$^-$ phosphido resonance form in N-heterocyclic phosphenium cations incorporated into a rigid pincer ligand framework.

Herein, we present a novel bidentate NHP$^+$/phosphine chelating ligand and its coordination to a series of d^{10} Ni fragments, demonstrating that the presence of two chelating phosphine arms is apparently a necessary requisite for the pyramidal NHP geometries previously observed with the tridentate NHP$^+$/diphosphine pincer ligand and group 10 metals.[8]

RESULTS AND DISCUSSION

Synthesis and Characterization. Synthesis of the diamine precursor to **1** was accomplished using a series of palladium cross coupling reactions in a procedure established by Stradiotto and co-workers.[9] Treatment of the diamine precursor with PCl_3 and three equivalents of NEt_3 in THF yielded the *N*-heterocyclic chlorophosphine ligand precursor [PP]-Cl (**1**) shown in Scheme 1. The ^{31}P NMR chemical shifts

Scheme 1

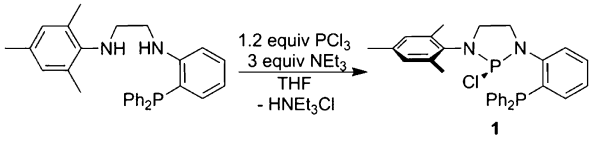

at −15.8 and 155.3 ppm for compound **1** are characteristic of triarylphosphine and *N*-heterocyclic chlorophosphine moieties, respectively (Figure 4). The molecular structure of **1** is shown in Figure 2.

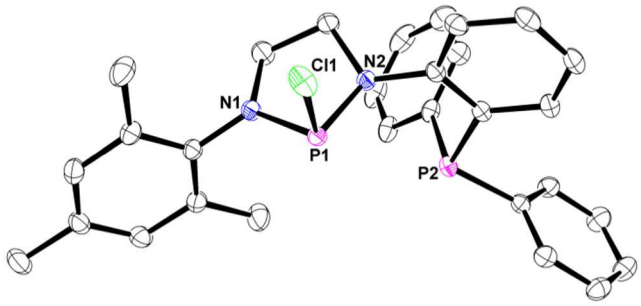

Figure 2. Displacement ellipsoid (50%) representation of **1**. For clarity, all hydrogen atoms have been omitted. Relevant interatomic distances (Å) and angles (deg): Cl1−P1, 2.2222(4); P1−N1, 1.6520(9); P1−N2, 1.6769(9); N1−P1−N2, 91.44(4).

Treatment of [PP]-Cl **1** with $Ni(COD)_2$ (COD = cyclooctadiene) in THF at 60 °C affords an asymmetric homobimetallic complex $[Cl_2Ni(\mu\text{-PP})_2Ni]$ (**2**), as shown in Scheme 2. The ^{31}P NMR spectrum of **2** features a downfield

Scheme 2

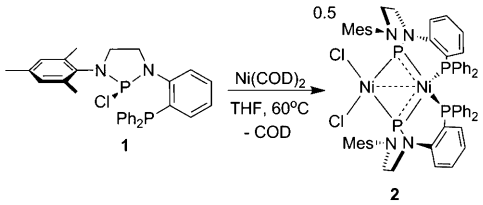

signal at 274.3 ppm for the NHP phosphorus atoms and an upfield signal at 23.6 ppm corresponding to the phosphine side arms (Table 1).

The solid state structure of **2** reveals an asymmetric NHP-bridged bimetallic Ni complex in which one Ni center is bound by the two triarylphosphine side arms, while the other is ligated by two chloride ions (Figure 3, Table 1). Each nickel center in complex **2** adopts a different coordination geometry: The geometry about the phosphine-bound Ni center (Ni1) is distorted tetrahedral (τ_4 = 0.79), whereas the chloride-bound Ni center (Ni2) adopts a distorted square planar geometry (τ_4 = 0.22) with the chloride atoms *trans* to the NHP moiety (where $\tau_4 = 360° - (\alpha - \beta)/141°$).[10] The phosphine-bound Ni1 center has short bond distances to both NHP phosphorus atoms (Ni1−P1, 2.0772(9) Å; Ni1−P3, 2.0825(9) Å), while the chloride-bound Ni2 center has elongated bonds to both NHP phosphorus atoms (Ni2−P1, 2.1993(10) Å; Ni2−P3, 2.1822(9) Å). The NHP moiety adopts a more planar geometry with respect to its interaction with the Ni1 center, with an angle of 155° between the N−P−N plane and the

DOI: 10.1021/acs.inorgchem.5b01363
Inorg. Chem. 2015, 54, 8717−8726

Table 1. Experimental M−P$^{(NHP)}$ Distances and ^{31}P NMR Chemical Shifts of Complexes 1−8 and a Selection of Comparable Metal NHP Complexes

compound	M−P$^{(NHP)}$ distance	P$^{(NHP)}$ ^{31}P NMR chemical shift (δ, ppm)
[PP]-Cl (**1**)	N/A	155.3
[PPP]-Cl[7]	N/A	147.9
[Cl_2Ni(μ-PP)$_2$Ni] (**2**)	2.0772(9) Å	274.3
	2.0825(9) Å	
[(PP)Ni(PP-F)]$^+$ (**3**)	2.0088(4) Å	256.8
	2.1167(4) Å	151.5
[(PP)Ni(COD)]$^+$ (**4**/**5**)	N/A	230
[(PP)Ni(PMe_3)$_2$]$^+$(**6**)	1.9840(4) Å	236.0
[(PP)Ni(PPh_3)$_2$]$^+$(**7**)[a]	2.0110(10) Å	227.5
	2.0098(8) Å	
[(PP-Cl)NiCl_2] (**8**)	2.0891(5) Å	106.9
[PPP]PdCl[2b]	2.2424(13) Å	248.6
[PPP]PtBr[2b]	2.2446(11) Å	246.1
{[PPP]Pt(PPh_3)}$^{+2b}$	2.2600(7) Å	198.8
{[PPP]Pt(PMe_3)}$^{+2b}$	2.2606(9) Å	205.5
{[PPP]Pd(PMe_3)}$^{+2b}$	2.2535(6) Å	235.6
(u^{Mes}NHP)Pd(Br)(PPh_3)$_2$[2e]	2.1166(17) Å	213.9
[(u^{Mes}NHP)Pd(PPh_3)$_2$]$^{+2e}$	2.1229(11) Å	213.0
(u^{Mes}NHP)Co(CO)$_3$[3b]	2.0018(4) Å	233.0
[(u^{Dipp}NHP)Fe(CO)$_3$]$^{-3e}$	1.989(1) Å	197.9
[(u^{Dipp}NHP)PdCl]$_2$[2g]	2.2738(4) Å	225.1
	2.2401(4) Å	
[(u^{Dipp}NHP)PtCl]$_2$[2g]	2.239(3) Å	26.9
	2.179(3) Å	
Co_2(CO)$_5$(μ-^{Me}NHP)$_2$[3c]	2.393(1) Å	307
	2.426(2) Å	
	2.051(1) Å	
	2.043(1) Å	
(^{Me}NHP)Ni(CO)$_3$[4]	N/A	274

[a]Distances for both molecules in the asymmetric unit of **7** are listed.

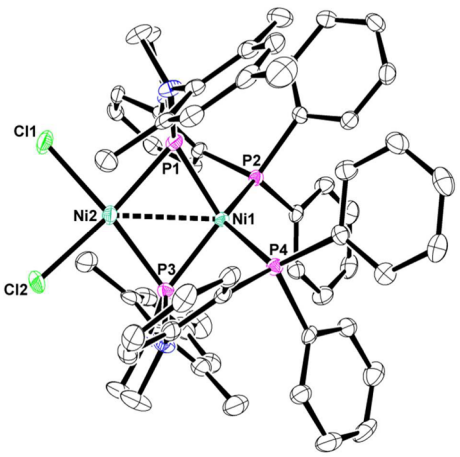

Figure 3. Displacement ellipsoid (50%) representation of **2**. For clarity, all hydrogen atoms and solvate molecules have been omitted. Relevant interatomic distances (Å) and angles (deg): Ni1−Ni2, 2.5523(5); Ni1−P1, 2.0772(9); Ni1−P3, 2.0825(9); Ni2−P1, 2.1993(10); Ni2−P3, 2.1822(9); Ni2−Cl1, 2.2353(9); Ni2−Cl2, 2.2452(9); Ni2−P1−Ni1, 73.22(3); Ni2−P3−Ni1, 73.48(3).

P$^{(NHP)}$−Ni1 bond vector. The angle between the N−P−N plane and the P$^{(NHP)}$−Ni2 bond vector is considerably more bent (131.6°). In combination with the short Ni1−P$^{(NHP)}$ distance, this implies that the Ni1−P$^{(NHP)}$ interaction in **2** is comprised of multiple bond character, with both P → Ni σ-donation and Ni → P π-backbonding. The chloride-bound Ni2, on the other hand, interacts with the two NHP phosphorus atoms in a weaker fashion.

The coordination of the [PP]$^+$ ligand to Ni^0 was also explored in the absence of halides. The free phosphenium ligand [PP]$^+$ could be generated *in situ* using halide abstraction agents such as $TlPF_6$, $NaBPh_4$, or K[B(C_6F_5)$_4$] but was found to be relatively unstable over time.[11] The ^{31}P NMR spectrum of [PP][PF_6] reveals two doublets at 143.0 and 3.1 ppm, with J_{PP} coupling of 430 Hz (Figure 4). In comparison to chlorophosphine **1**, the upfield shift of the resonance for the NHP$^+$ phosphorus atom, the downfield shift of the phosphine side arm, and the substantial increase in J_{PP} coupling constant indicate an intramolecular R_3P → P^{NHP} interaction, as also observed for the free [PPP]$^+$ pincer ligand.[7] Owing to the insability of [PP]$^+$, it was not isolated and was generated *in situ* for all further studies of its coordination chemistry to Ni^0.

The treatment of **1** with 1 equiv of $TlPF_6$ in CH_2Cl_2, followed by the addition of 0.5 equiv of Ni(COD)$_2$ afforded the doubly ligated [(PP)Ni(PP-F)][PF_6] (**3**, Scheme 3). The ^{31}P NMR spectrum of **3** features four distinct [PP]$^+$-derived signals, including a diagnostic broad singlet at 256.8 ppm corresponding to a halide-free NHP phosphorus atom (Table 1). An additional doublet of doublet of doublets is observed at 151.5 ppm, with a large $^1J_{PF}$ coupling constant of 1155 Hz and $^2J_{PP}$ coupling constants of 95 and 42 Hz. The large $^1J_{PF}$ and upfield chemical shift are indicative of fluoride abstraction by one of the electrophilic NHP$^+$ phosphorus atoms. Two resonances for the Ni-bound phosphorus side arms of the two inequivalent [PP]$^+$-derived ligands are observed as a broad singlet at 24.5 ppm and an overlapping doublet of doublets at 20.1 ppm. The latter signal is assigned to the phosphine side arm of the [PP-F] ligand, with $^2J_{PP}$ and $^3J_{PF}$ coupling constants of 43 and 95 Hz, respectively.

As expected from the spectroscopic features, the solid state structure of **3** (Figure 5) reveals a structure with two bidentate ligands in which one of the NHP$^+$ phosphorus atoms has abstracted a fluoride ion from the PF_6^- anion. The Ni center in complex **3** adopts a distorted tetrahedral coordination geometry (τ_4 = 0.79).[10] The NHP$^+$ phosphenium ligand adopts a nearly planar coordination mode with the sum of the three angles about phosphorus equal to 357.0°. Multiple bond character is also reflected by the short Ni−P1 distance of 2.0088(4) Å (Table 1). While there are no structurally characterized NHP$^+$ Ni complexes reported in the literature for comparison, the P$^{(NHP)}$−Ni bond distance in **3** is similar to the P$^{(NHP)}$−M distances in [CpFe(CO)($SiMe_3$)(^{Me}NHP)][BPh_4], (u^{Mes}NHP)Co(CO)$_3$, (u^{tBu}NHP)Co(CO)$_3$, and [u^{Dipp}NHP-Fe(CO)$_3$][PPh_4] (Dipp = 2,6-diisopropylphenyl), which represent the only structurally characterized NHP$^+$ complexes of first row transition metals to date (2.018(2) Å, 2.0018(4) Å, 2.0450(5) Å, and 1.989(1) Å, respectively).[3b,e,g] In contrast, the NHP-derived fluorophosphine ligand is bound more weakly to Ni, as reflected by the longer Ni−P3 distance of 2.1167(4) Å.

In an effort to avoid halide abstraction from the counteranion, the more robust noncoordinating counterions [B(C_6F_5)$_4$]$^-$ and [BPh_4]$^-$ were used. Abstraction of the chloride anion from **1** with K[B(C_6F_5)$_4$], followed by immediate coordination to Ni using 0.5 equiv of Ni(COD)$_2$ in an effort to isolate a dicationic bis(phosphenium) complex

DOI: 10.1021/acs.inorgchem.5b01363
Inorg. Chem. 2015, 54, 8717−8726

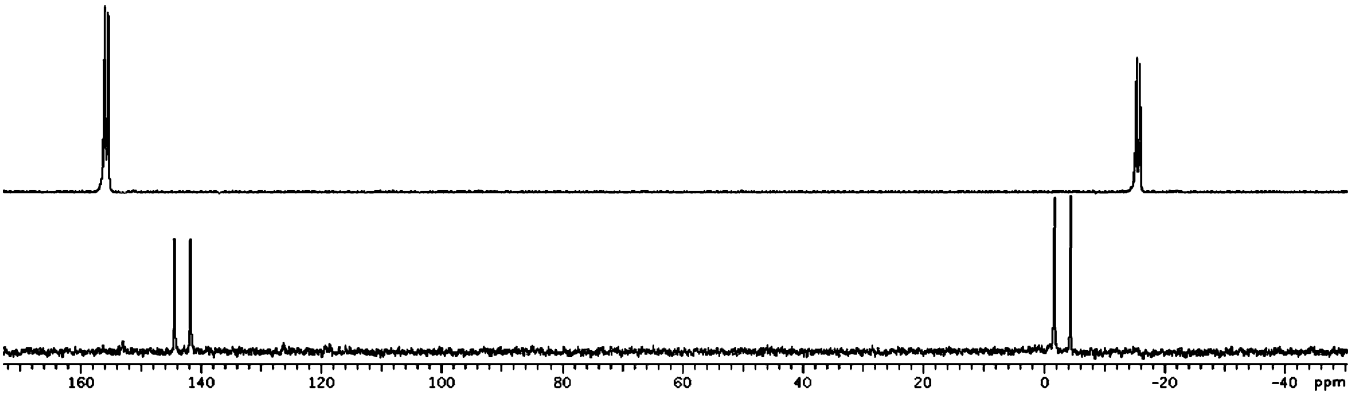

Figure 4. $^{31}P\{^{1}H\}$ NMR spectra of **1** (top) and [PP][PF_6] generated *in situ* via addition of $TlPF_6$ to **1** (bottom) in CH_2Cl_2. The resonance associated with the PF_6^- counterion is not shown (see Supporting Information for full spectrum).

Scheme 3

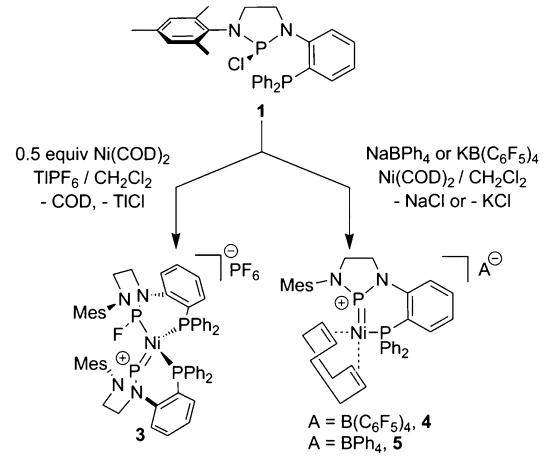

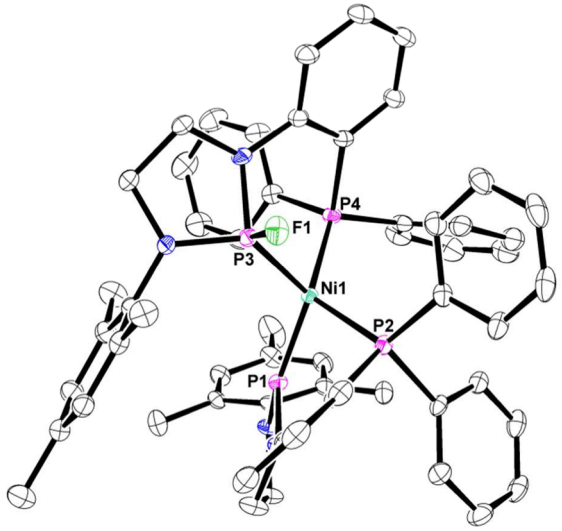

Figure 5. Displacement ellipsoid (50%) representation of **3**. For clarity, all hydrogen atoms, the PF_6^- counteranion, and solvate molecules have been omitted. Relevant interatomic distances (Å): Ni1−P1, 2.0088(4); Ni1−P3, 2.1167(4); P3−F1, 1.6189(10).

$[(PP)_2Ni][B(C_6F_5)_4]_2$ results in a mixture of inseparable products including two Ni-phosphenium complexes with ^{31}P NMR resonances at 265.3 and 231.2 ppm (Figure S20) and the free $[PP]^+$ ligand (142 ppm (d)). However, the absence of additional ^{31}P NMR signals in the 100−150 ppm range in this reaction mixture confirms that no anion abstraction from the counterions has occurred.

In contrast, treatment of *in situ*-generated [PP][$B(C_6F_5)_4$] or [PP]BPh_4 with stoichiometric $Ni(COD)_2$ led to exclusive formation of the monosubstituted complexes [(PP)Ni(COD)]-[$B(C_6F_5)_4$] (**4**) and [(PP)Ni(COD)][BPh_4] (**5**), respectively (Scheme 3). The ^{31}P NMR spectra of **4** and **5** are identical, with a downfield signal at 230 ppm for the phosphenium moiety and an upfield signal at 12 ppm for the phosphine side arm (Table 1). The ^{1}H NMR spectra of complexes **4** and **5** feature 10 signals between 1 and 6 ppm, suggesting a Ni-bound COD molecule is present in an asymmetric environment. A 2-D homonuclear total correlation spectroscopy (TOCSY) experiment confirmed the identity of the six COD-derived resonances and identified the two CH_2 signals corresponding to the NHP^+ ligand backbone at 3.72 and 4.04 ppm (Figures S17, S18). Single crystals of **4** or **5** suitable for X-ray diffraction could not be obtained.

The COD ligand in **5** is easily displaced by added tertiary phosphine ligands. The addition of PMe_3 or PPh_3 to **5** leads to facile displacement of the diene to afford [(PP)Ni(PMe_3)$_2$]-[BPh_4] (**6**) and [(PP)Ni(PPh_3)$_2$][BPh_4] (**7**), respectively (Scheme 4). The ^{31}P NMR spectrum of **6** features signals at

Scheme 4

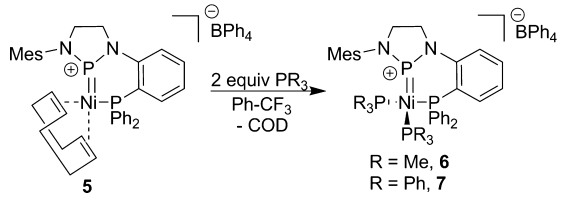

236.0 ppm, 18.8 ppm, and −17.4 ppm, representing the NHP^+ phosphorus atom, the phosphine side arm, and the PMe_3 ligand, respectively (Table 1). Similarly, signals at 227.5 ppm (NHP^+), 34.0 ppm (PPh_3), and 10.7 ppm (side arm) are present in the ^{31}P NMR spectrum of complex **7**.

The solid state structures of **6** and **7**, shown in Figure 6, have similar tetrahedral geometries about the Ni centers with τ_4 values of 0.88 and 0.89, respectively.[10] In both complexes, the NHP^+ ligand adopts a planar binding mode, with the angles about the phosphorus atom summing to 360.0° in both complexes **6** and **7**. The $P^{(NHP)}$−Ni bonds of complexes **6** and **7** (1.9840(4) Å and 2.0108(10) Å [2.0098(8) Å])[12] are short and

DOI: 10.1021/acs.inorgchem.5b01363
Inorg. Chem. 2015, 54, 8717−8726

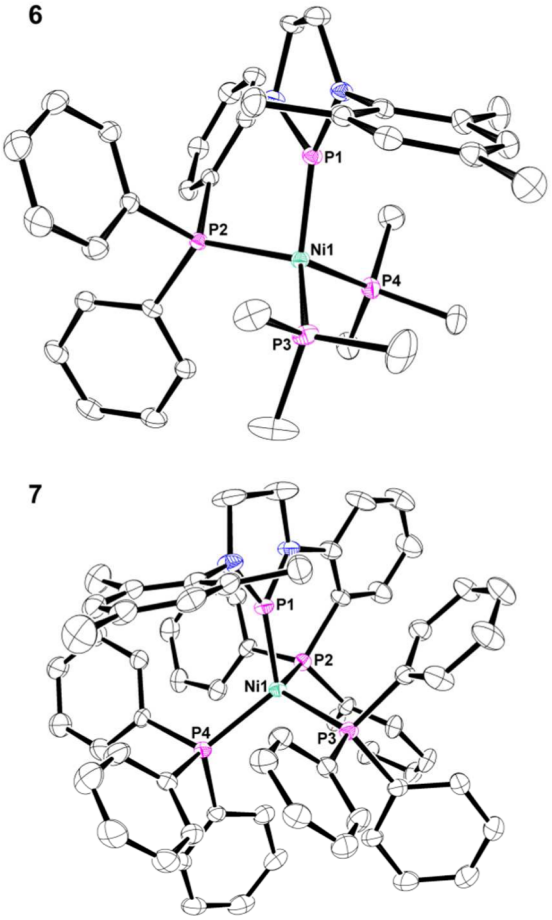

Figure 6. Displacement ellipsoid (50%) representation of complexes **6** (top) and **7** (bottom). For clarity, all hydrogen atoms and the $BPh4^-$ counteranions have been omitted. There are two similar independent molecules in the asymmetric unit of **7**. Only one molecule is shown for clarity, but the distances for the second molecule are listed in brackets. Relevant interatomic distances (Å), **6**: Ni1–P1, 1.9840(4); Ni1–P2, 2.1722(4); Ni1–P3, 2.2030(4); Ni1–P4, 2.2105(4); P1–N1 = 1.6351(11); P1–N2 = 1.6690(11). **7**: Ni1–P1, 2.0110(10) [2.0098(8)]; Ni1–P2, 2.220(7) [2.2221(8)]; Ni1–P3, 2.2381(8) [2.2446(8)]; Ni1–P4, 2.2425(7) [2.2341(8)].

indicative of Ni–P double bond character (Table 1). In fact, the $P^{(NHP)}$–Ni bond distance in **6** is among the shortest metal–phosphorus distances reported for metal phosphenium complexes and is very similar to the $P^{(NHP)}$–Fe bond distance of 1.989(1) Å in $[(u^{Dipp}NHP)Fe(CO)_3][PPh_4]$.[3e] Furthermore, based on a search of the Cambridge Structural Database (CSD), complexes **3**, **6**, and **7** contain the shortest Ni–P distances reported to date and are even shorter than the Ni–P multiple bond distances in Hillhouse's Ni-phosphido and phosphinidene complexes $[(dtbpe)Ni{=}P(H)(dmp)][PF_6]$ and $[(dtbpe)Ni{=}P(dmp))]$ (dtbpe = 1,2-(di-*tert*-butylphosphino)ethane and dmp = 2,6-dimesitylphenyl), which are 2.0540(11) Å and 2.0772(9) Å, respectively.[13]

The planar binding mode of the NHP ligand in **6** and **7** is in stark contrast to the pyramidal geometry of the NHP ligand in the cationic tris(phosphine)-ligated Pd and Pt NHP complexes $[PPP]M(PR_3)^+$ previously reported by our group.[2b] The obvious difference between the complexes is the ability of one *N*-aryl substituent to freely rotate in complexes **6** and **7**, but a question arises as to whether *N*-aryl orientation affects delocalization of the nitrogen lone pair or whether steric effects are at play. We note that the P–N distance associated with the mesityl-substituted nitrogen atom is shorter in both **6** and **7** than the P–N distance associated with the aryl group of the chelating side arm (P1–N1 = 1.6351(11) Å vs P1–N2 = 1.6690(11) Å for **6**; P1–N1 = 1.646(3) Å [1.646(3) Å] vs P1–N2 = 1.678(3) Å [1.671(3) Å] for **7**). This suggests more P–N π donation from the mesityl-substituted nitrogen atom and is consistent with the hypothesis that diminished *N*-aryl π delocalization leads to the different geometries adopted by the NHP fragments of the $[PP]^+$ and $[PPP]^+$ ligands in otherwise analogous complexes.

In addition to Ni^0 coordination, we also explored the metalation of ligand precursor **1** with a Ni^{II} precursor. Perhaps not surprisingly, when $Ni(DME)Cl_2$ (DME = dimethoxyethane) was treated with **1**, P–Cl bond cleavage was not observed and the chlorophosphine coordination complex $[(PP\text{-}Cl)NiCl_2]$ (**8**) was formed exclusively (Scheme 5). The ^{31}P

Scheme 5

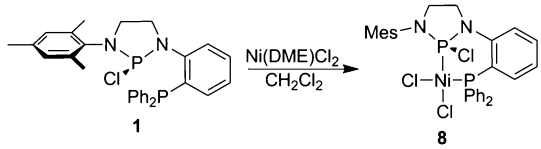

NMR spectrum of **8** has an upfield signal at 106.9 ppm, with no signals further downfield, indicating that the P–Cl bond remains intact. A second ^{31}P NMR signal is observed at 12.6 ppm for the Ni-bound phosphine side arm. The solid state structure of **8** confirms the connectivity suggested by the ^{31}P NMR data (Figure 7) and reveals that, in contrast to Ni^0

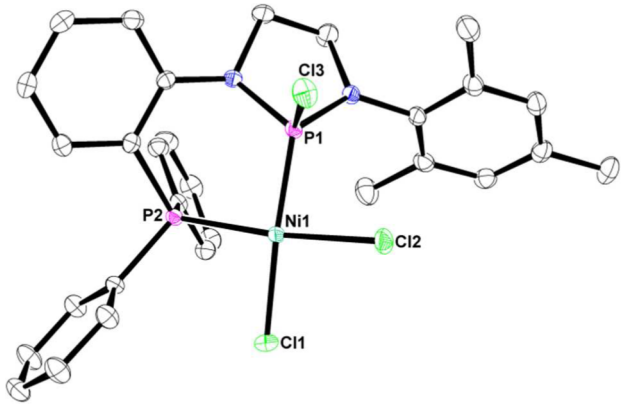

Figure 7. Displacement ellipsoid (50%) representation of **8**. For clarity, all hydrogen atoms have been omitted. Relevant interatomic distances (Å): Ni1–P1, 2.0891(5); Ni1–P2, 2.1688(5), Ni1–Cl1, 2.1742(5); Ni1–Cl2, 2.1903(5); Cl3–P1, 2.0849(6).

complexes **3**–**7**, the geometry about the Ni center in **8** is rigorously square planar (τ_4 = 0.09). The P1–Ni distance of 2.0891(5) Å is elongated compared to the NHP^+ phosphenium Ni complexes described previously (Table 1) but is significantly shorter than the Ni–P distance associated with the phosphine side arm (2.1688(5) Å) as a result of the well-documented ability of halophosphines to engage in π-backbonding. A similar trend in M–P distances is observed in our previously reported Pt^{II} chlorophosphine complex $[(PPP\text{-}Cl)PtCl][PF_6]$.[7] Attempts to abstract a chloride anion from complex **8** using $K[B(C_6F_5)_4]$

DOI: 10.1021/acs.inorgchem.5b01363
Inorg. Chem. 2015, 54, 8717–8726

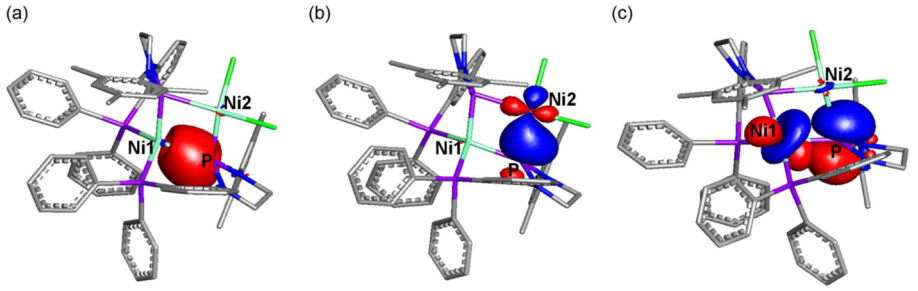

Figure 8. Visual representations of the calculated Ni–P bonding interactions in complex **2** using natural bond orbital (NBO) analysis: (a) $P^{(NHP)}$–Ni1 NBO; (b) $P^{(NHP)}$–Ni2 NBO; (c) donor–acceptor interaction between a Ni1-based lone pair and an empty phosphorus p orbital.

Table 2. Computed Ni and $P^{(NHP)}$ Natural Charges, Ni Natural Electron Configurations, and Composition of Ni–$P^{(NHP)}$ Natural Bond Orbitals for Complexes 2, $[(PP)Ni(COD)]^+$, and 6[a]

	natural charges			Ni–$P^{(NHP)}$ NBO composition	
	Ni	$P^{(NHP)}$[b]	Ni natural electron configuration	Ni	P
$[Cl_2Ni(\mu\text{-}PP)_2Ni]$ **2**	−0.98 (Ni1)	1.47	$4s^{0.37}3d^{9.34}4p^{1.27}$ (Ni1)	23.5% (24% s, 74% p)	76.5% (45% s, 55% p)
	−0.17 (Ni2)	1.47	$4s^{0.31}3d^{9.18}4p^{0.15}$ (Ni2)	61.6% (3% s, 9% p, 88% d)	38.4% (20% s, 80% p)
$[(PP)Ni(COD)]^+$ (**4**/**5**)	−0.42	1.48	$4s^{0.29}3d^{9.25}4p^{0.23}$	19.3% (25% s, 74% p)	80.7% (63% s, 37% p)
$[(PP)Ni(PMe_3)_2]^+$ (**6**)	−1.00	1.49	$4s^{0.44}3d^{9.32}4p^{1.24}$	20.8% (24% s, 75% p)	79.2% (64% s, 36% p)

[a]Computed using DFT geometry optimizations and subsequent NBO analysis (B3LYP/LANL2DZ). [b]Natural charges for the phosphorus atoms of Ni-bound phosphines are in the range of 1.05–1.12 for all three complexes.

were unsuccessful, as no reaction occurred at room temperature over 18 h (Figure S21).

Computational Investigation. To better understand the bonding in the series of new nickel NHP complexes, a computational investigation was carried out using Density Functional Theory (DFT). Geometry optimizations and subsequent natural bond orbital (NBO) calculations were performed on the untruncated molecules **2**, $[(PP)Ni(COD)]^+$, and **6** starting from the crystallographic coordinates.

The best Lewis structure of **2** found by NBO analysis consists of a bimetallic $Ni_2[PP]_2^{2+}$ dication interacting weakly with two independent Cl^- anions (Figure S29). It was found that the Ni1–$P^{(NHP)}$ NBOs in complex **2** (Figure 8a) are strongly polarized toward the phosphorus atom (23.5% Ni1, 76.5% P) with atomic contributions similar to the Ni–P NBOs associated with the phosphine side arms (20.6% Ni2, 79.4% P) indicating similar donation of the phosphorus lone pairs to the phosphine-ligated Ni1 center (Table 2). However, the Ni1–$P^{(NHP)}$ NBOs are comprised of substantially more phosphorus s character compared to the typical 25% s/75% p character of a tertiary phosphine lone pair. In addition to the σ bonds, second order perturbation theory reveals donor–acceptor interactions from the Ni1-based lone pairs (96% d character) into the empty phosphorus p orbitals (98% p character) with a 25 kcal/mol stabilization energy (Figure 8c). These interactions represents π-back-donation from the Ni1 center to the NHP ligands. This σ-donor + π-acceptor character is consistent with the contracted Ni1–P distance observed in the solid state structure of **2**. In contrast, the Ni2–$P^{(NHP)}$ NBOs feature a greater contribution from the Ni2 center (61.6% Ni2, 38.4% P), and the orbital compositions are indicative of donation from a filled d orbital on the chloride-bound Ni2 center into the empty p orbitals on the NHP phosphorus atoms (Figure 8b, Table 2). These bonding descriptions lead to the assignment of complex **2** as a dinickel(0) complex asymmetrically bridged by two NHP^+ cations. Consistent with the Ni^0 formal oxidation state assignment, the natural electron configuration of both Ni centers is close to d^{10} with fewer d electrons on Ni2 as a result of Ni → P donation and additional p electrons on Ni1 as a result of P → Ni donation (Table 2). Computed natural charges, indeed, show Ni1 to be more electron-rich than Ni2 and the NHP phosphorus to be more positively charged than a typical phosphine phosphorus atom or the pyramidal NHP phosphorus atoms in group 10 [PPP] pincer-ligated complexes.[2b] In addition, the sum of the natural charges on each $[PP]^+$ ligand fragment is +1.07 (Table S3).

Thus, unlike the products of the reactions of the tridentate pincer-based [PPP-Cl] ligand and group 10 metal(0) precursors such as [PPP]PdCl,[2b] a formal oxidative addition of the P–Cl bond to the metal center has not occurred, and both Ni centers remain in the Ni^0 oxidation state in the NHP^+ phosphenium-bridged complex **2**. Similar "non-oxidative additions" of *N*-heterocyclic chlorophosphines have been described for Pd^0, Pt^0, and Ni^0,[2e,i,5] and a metal(0)/phosphenium formalism has also been postulated for several monodentate NHP metal halide complexes including $[(u^{Dipp}NHP)MCl]_2$ (M = Pd, Pt)[2g] and $(u^{Mes}NHP)Pd(Br)(PPh_3)_2$.[2e] The asymmetric bridging motif in complex **2** is similar to that described by Baker for the asymmetric NHP-bridged bimetallic Ni complex $[(\mu\text{-}^{Mes}NHP)NiCl]_2$,[5] as well as the dinuclear cobalt complex $Co_2(CO)_5(\mu\text{-}^{Me}NHP)_2$ described by Paine.[3c]

The bonding in monomeric complex **6** is less complicated owing to interaction of the NHP phosphorus atom with just one Ni center. NBO calculations conducted on complex **6** also reveal a Ni–P multiple bond comprised of both P → Ni σ donation and Ni → P π-backbonding (Figure 9). The $P^{(NHP)}$–Ni NBO is strongly polarized toward the phosphorus atom (20.80% Ni, 79.20% P), again indicative of donation from the phosphorus lone pair to Ni (Table 2). In addition to σ donation, a donor/acceptor interaction from a lone pair on Ni (95% d character) to an empty phosphorus p orbital (99% p character) was identified by second order perturbation theory, with a stabilization energy of 105.6 kcal/mol. This interaction

DOI: 10.1021/acs.inorgchem.5b01363
Inorg. Chem. 2015, 54, 8717–8726

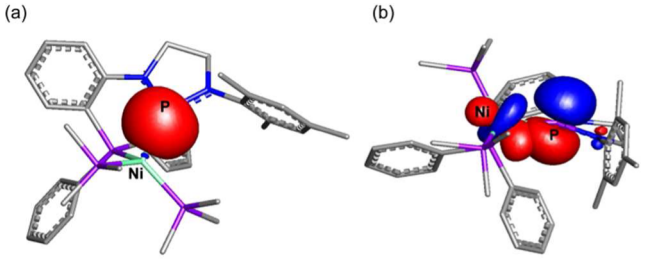

Figure 9. Visual representations of the Ni−P bonding interactions in complex **2** calculated using natural bond orbital (NBO) analysis: (a) $P^{(NHP)}$−Ni NBO; (b) donor−acceptor interaction between a Ni-based lone pair and an empty phosphorus p orbital.

corresponds to additional π-backbonding from the Ni center to the NHP ligand. The combination of these two interactions is consistent with the short Ni−P distance in this complex and with an NHP^+/Ni^0 assignment. The computed Ni and $P^{(NHP)}$ natural charges and electron configuration of the Ni center in complex **6** are nearly identical to those associated with the Ni1 center in bimetallic complex **2**, and the total natural charge of +0.84 on the $[PP]^+$ ligand in **6** is slightly lower as a result of stronger π-back-donation from Ni (Table S7).

Since crystals of **4** or **5** suitable for X-ray diffraction could not be obtained, DFT calculations were used to evaluate the geometry and bonding in the $[(PP)Ni(COD)]^+$ ion (Figures S28 and S30). The optimized geometry of $[(PP)Ni(COD)]^+$ reveals a distorted tetrahedral geometry about the Ni center (τ_4 = 0.75) and a planar NHP^+ binding mode quite similar to the structurally characterized analogues **6** and **7**. The results of NBO calculations on $[(PP)Ni(COD)]^+$ suggest very similar $Ni-P^{NHP}$ bonding (Table 2).

CONCLUSION

In summary, incorporation of an *N*-heterocyclic phosphenium (NHP^+) cation into a bidentate chelating ligand framework has permitted the isolation of the first structurally characterized examples of coordination complexes of NHP^+ ligands with Ni. The addition of the *N*-heterocyclic chlorophosphine precursor to Ni^0 leads to the addition of the $P^{(NHP)}$−Cl bond to Ni in a non-oxidative fashion, affording a bimetallic Ni^0 complex. Monometallic cationic nickel phosphenium NHP^+ complexes $[(PP)NiL_2]^+$ can be synthesized via direct coordination of the $[PP]^+$ ligand to Ni^0. These compounds feature the shortest reported Ni−P distances ever reported, highlighting the Ni−P multiple bond character resulting from σ-donation and strong Ni → P π-backbonding.

The new bidentate ligand framework also allows us to interrogate the origin of the unusual pyramidal NHP geometries previously observed when a similar tridentate NHP^+/diphosphine pincer ligand was coordinated to group 10 metals.[7] We had previously attributed this behavior to the rigid pincer framework forcing a coplanar orientation of the *N*-aryl rings with the *N*-heterocycle, allowing delocalization of the nitrogen lone pairs into the aromatic ring rather than stabilizing the empty p orbital on the central phosphorus. As a result, the more electron-poor phosphorus center of the $[PPP]^+$ pincer ligand formally oxidizes low valent group 10 metal centers to become a pyramidal *N*-heterocyclic phosphido (NHP^-) with a stereochemically active lone pair.

In the case of the bidentate $[PP]^+$ ligand reported here, however, only one aryl ring is rigidly locked in position by the chelating side arm, and the other *N*-aryl group is allowed to freely rotate to a position perpendicular to the plane of the heterocycle as is typical in monodentate NHP^+ (and NHC) ligands. This leads to a planar NHP^+ binding mode in the case of the bidentate $[PP]^+$ chelating ligand. Therefore, we suggest that allowing one aryl ring to freely rotate permits more stabilization of the phosphenium cation via N−P π delocalization and allows it to coordinate to d^{10} metal centers without formally oxidizing the metal center and adopting a pyramidal NHP^- phosphido geometry. Admittedly, it is also possible that the observed unusual pyramidal coordination behavior of the $[PPP]^+$ pincer ligand is a consequence of geometric constraints imposed by the rigid pincer framework and that removal of one of the phosphine side arms alleviates these constraints.

Further investigations will focus on the reactivity of these Ni complexes, as well as further explorations of the coordination chemistry of NHP^+ ligands using the NHP^+/phosphine bidentate ligand.

EXPERIMENTAL SECTION

General Considerations. Unless specified otherwise, all manipulations were performed under an inert atmosphere using standard Schlenk or glovebox techniques. Glassware was oven-dried before use. N-pentane, tetrahydrofuran, toluene, diethyl ether, and dichloromethane were degassed and dried by sparging with ultrahigh purity argon gas followed by passage through a series of drying columns using a Seca Solvent System by Glass Contour. All solvents were stored over 3-Å molecular sieves. Deuterated solvents were purchased from Cambridge Isotope Laboratories, Inc., degassed via repeated freeze−pump−thaw cycles, and dried over 3-Å molecular sieves. Solvents were frequently tested using a standard solution of sodium benzophenone ketyl in tetrahydrofuran to confirm the absence of oxygen and moisture. Ligand precursor (N^1-[2-(PPh_2)phenyl]-N^2-Mes-1,2-ethanediamine)[9] and $Ni(DME)Cl_2$[14] were synthesized using literature procedures. All other chemicals were purchased from Aldrich, Strem, or Alfa Aesar and used without further purification. NMR spectra were recorded at ambient temperature on a Varian Inova 400 or 400MR 400 MHz instrument. Chemical shifts are reported in δ (ppm). For ^1H and ^{13}C NMR spectra, the solvent resonance was used as an internal reference. For ^{31}P NMR spectra, 85% H_3PO_4 was referenced as an external standard (0 ppm), and ^{19}F NMR chemical shifts were referenced to CF_3CO_2H (−76.55 ppm). UV−vis spectra were recorded on a Cary 50 UV−vis spectrophotometer using Cary WinUV software. Elemental analyses were performed at Complete Analysis Laboratory Inc., Parsippany, New Jersey.

Synthesis of [PP]-Cl (1). N^1-[2-(PPh_2)phenyl]-N^2-Mes-1,2-ethanediamine (1.12 g, 2.55 mmol) was dissolved in 50 mL of THF with PCl_3 (0.51 mL 3.1 mmol), and to this solution was added Et_3N (2.0 mL, 7.7 mmol) dropwise. The reaction mixture immediately became cloudy but was allowed to stir overnight to ensure a complete reaction. The solvent was removed in vacuo, and the remaining residue was extracted into 60 mL of toluene and filtered through Celite. The solvent was removed from the filtrate in vacuo, and the residue was washed with an additional 20 mL of Et_2O to remove remaining impurities, leaving **1** as an off-white powder. X-ray quality crystals were obtained from a concentrated solution of **1** in toluene. Yield: 1.21 g, 95%. ^1H NMR (400 MHz, CD_2Cl_2): δ 7.58 (br, 1H, Ar-*H*), 7.47 (dd, 1H, $^3J_{HH}$ = 7.4 Hz, Ar-*H*), 7.37 (br, 6H, P-Ar-*H*), 7.31 (br, 4H, P-Ar-*H*), 7.19 (dd, 1H, $^3J_{HH}$ = 7.4 Hz, Ar-*H*), 6.93 (br, 3H, Ar-*H*, Mes-H), 4.18 (br, 1H, CH_2), 3.59 (m, 1H, CH_2), 3.44 (m, 1H, CH_2), 3.09 (br, 1H, CH_2), 2.49 (s, 3H, CH_3), 2.29 (br, 6H, CH_3). $^{31}P\{^1H\}$ NMR (161.8 MHz, CD_2Cl_2): δ 155.3 (d, 1P, $^2J_{P-P}$ = 94.8 Hz), −15.8 (d, 1P, $^2J_{P-P}$ = 94.8 Hz). $^{13}C\{^1H\}$ NMR (100.5 MHz, CD_2Cl_2): δ 145.6 (dd, $^3J_{CP}$ = 7.6 Hz, $^2J_{CP}$ = 20.0 Hz), 138.5 (s), 137.9 (d, $^2J_{CP}$ = 12.4 Hz), 137.6 (s), 137.5 (s), 136.9 (d, $^3J_{CP}$ = 11.4 Hz), 135.8 (d, $^3J_{CP}$ = 11.4 Hz), 138.5 (d, $^2J_{CP}$ = 14.3 Hz), 134.7 (s), 134.5 (s), 134.1 (d, J_{CP} =

DOI: 10.1021/acs.inorgchem.5b01363
Inorg. Chem. 2015, 54, 8717−8726

41.9 Hz), 134.0 (s), 130.3 (s), 129.7 (d, J_{CP} = 41.9 Hz), 129.1 (d, $^3J_{CP}$ = 4.8 Hz), 128.8 (dd, $^3J_{CP}$ = 6.7 Hz, $^2J_{CP}$ = 14.3 Hz), 126.8 (s), 125.5 (d, $^3J_{CP}$ = 3.8 Hz), 52.6 (d, $^3J_{CP}$ = 7.6 Hz), 51.6 (d, $^3J_{CP}$ = 8.6 Hz), 21.0 (s), 18.9 (s). Anal. Calcd for $C_{29}H_{29}N_2P_2Cl$: C, 69.25; H, 5.81; N, 5.57. Found: C, 69.15; H, 5.69; N, 5.40.

*Synthesis of [Cl_2Ni(μ-PP)$_2$Ni] (**2**).* Compound **1** (54 mg, 0.11 mmol) was dissolved in 5 mL of THF, and to this light yellow solution was added Ni(COD)$_2$ (30 mg, 0.11 mmol). The mixture was stirred and heated to 60 °C. After 20 min, the reaction was allowed to cool to room temperature, and all the volatiles were removed in vacuo. The resulting brown residue was washed once with 5 mL of Et_2O and dried in vacuo to yield analytically pure product as a brown solid. Crystals suitable for X-ray crystallography were grown via layering pentane onto a concentrated CH_2Cl_2 solution of **2**. Yield: 111 mg, 91%. ^{1}H NMR (400 MHz, $CDCl_3$): δ 7.53 (m, 2H, Ar-*H*), 7.44 (dd, 2H, $^3J_{HH}$ = 7.3 Hz, Ar-*H*), 7.32 (m, 4H, P-Ar-*H*), 7.09 (m, 8H, P-Ar-*H*), 6.99 (br, 4H, P-Ar-*H*), 6.85 (dd, 2H, $^3J_{HH}$ = 7.0 Hz, Ar-*H*), 6.72 (s, 2H, Mes-*H*), 6.50 (br, 4H, P-Ar-*H*), 6.42 (s, 2H, Mes-*H*), 5.76 (m, 2H, Ar-*H*), 4.74 (br, 2H, CH_2), 4.37 (m, 2H, CH_2), 3.45 (m, 2H, CH_2), 3.29 (br, 2H, CH_2), 2.26 (s, 6H, CH_3), 2.05 (s, 6H, CH_3), 1.49 (s, 6H, CH_3). ^{31}P{^{1}H} NMR (161.8 MHz, $CDCl_3$): δ 274.3 (s), 23.6 (s). ^{13}C{^{1}H} NMR (100.5 MHz, $CDCl_3$): δ 144.7 (m), 138.5 (s), 137.2 (m), 135.7 (m), 135.6 (s), 134.8 (s), 132.6 (m), 130.8 (s), 130.7 (m), 129.8 (s), 129.4 (s), 129.3 (s), 129.1 (m), 128.0 (s), 127.9 (s), 125.8 (m), 123.3 (s), 122.9 (s), 51.3 (s), 47.2 (s), 22.3 (s), 20.8 (s), 17.5 (s). UV−vis (CH_2Cl_2, λ (nm) (ε, M^{-1} cm^{-1})): 485 (3.51 × 10^3). Anal. Calcd for $C_{58}H_{58}N_4P_4Cl_2Ni_2$: C, 62.02; H, 5.20; N, 4.99. Found: C, 61.85; H, 5.01; N, 4.78.

*Synthesis of [(PP)Ni(PP-F)][PF_6] (**3**).* Compound **1** (50 mg, 0.99 mmol) was dissolved in 5 mL of CH_2Cl_2, and to this light yellow solution was added $TlPF_6$ (35 mg, 0.99 mmol). The mixture was allowed to stir at room temperature for 12 h. The reaction mixture was filtered through Celite and then was added to Ni(COD)$_2$ (14 mg, 0.50 mmol), and the resulting mixture was allowed to stir for an additional 6 h. The dark purple mixture was then filtered through Celite, and the volatiles were removed from the dark purple filtrate in vacuo, affording analytically pure product as a purple solid. Crystals suitable for X-ray crystallography were grown via layering Et_2O onto a concentrated THF solution of **3**. Yield: 99 mg, 86%. ^{1}H NMR (400 MHz, CD_2Cl_2): δ 7.69 (dd, 1H, $^3J_{HH}$ = 7.4 Hz, Ar-*H*), 7.56−7.48 (m, 2H, Ar-*H*), 7.42−7.02 (m, 22H, Ar-*H*), 6.91−6.85 (m, 2H, Mes-Ar-*H*, Ar-*H*), 6.81 (s, 1H, Mes-Ar-*H*), 6.69 (s, 1H, Mes-Ar-*H*), 6.45−6.38 (m, 3H, Mes-Ar-*H*, Ar-*H*), 4.15 (m, 1H, CH_2), 3.81−3.68 (m, 3H, CH_2), 3.51 (m, 1H, CH_2), 3.38 (br, 1H, CH_2), 3.15 (m, 2H, CH_2), 2.40 (s, 3H, CH_3), 2.36 (s, 3H, CH_3), 2.22 (s, 3H, CH_3), 1.44 (s, 3H, CH_3), 1.33 (s, 3H, CH_3), 0.93 (s, 3H, CH_3). ^{31}P{^{1}H} NMR (161.8 MHz, CD_2Cl_2): δ 256.8 (br s, 1P), 151.5 (ddd, 1P, $^1J_{PF}$ = 1160 Hz, $^2J_{PP}$ = 95 Hz, 42 Hz), 24.5 (br s, 1P), 20.1 (overlapping dd, 1P, $^2J_{PP}$ = 43 Hz, $^3J_{PF}$ = 95 Hz), −143.8 (sept, 1P, $^1J_{PF}$ = 711 Hz, PF_6^-). ^{19}F{^{1}H} NMR (376 MHz, CD_2Cl_2): δ −20.7 (dm, 1F, $^1J_{PF}$ = 1160 Hz), −74.3 (d, 6F, $^1J_{PF}$ = 710 Hz, PF_6^-). ^{13}C{^{1}H} NMR (100.5 MHz, CD_2Cl_2): δ 146.2 (m), 144.0 (m), 139.8 (s), 139.7 (s), 137.4 (s), 137.2(s), 136.9 (d, $^2J_{CP}$ = 16.2 Hz), 136.8 (m), 136.5 (m), 135.7 (d, $^2J_{CP}$ = 16.2 Hz), 135.3 (d, $^2J_{CP}$ = 15.3 Hz), 134.1 (d, $^2J_{CP}$ = 15.3 Hz), 133.4 (s), 133.1 (d, $^2J_{CP}$ = 15.3 Hz), 132.4 (s), 131.8 (s), 131.7 (s), 131.5 (s), 130.5 (s), 130.4 (s), 130.3 (s), 130.1 (d, $^3J_{CP}$ = 5.7 Hz), 129.5 (s), 129.3 (s), 129.0 (d, $^3J_{CP}$ = 7.6 Hz), 128.8 (s), 128.7 (d, $^3J_{CP}$ = 9.5 Hz), 128.5 (s), 125.7 (d, $^3J_{CP}$ = 6.7 Hz), 125.6 (s), 124.2 (m), 120.7 (dm, $^1J_{CP}$ = 32.4 Hz), 51.0 (s), 49.7 (s), 48.4 (s), 47.2 (s), 21.1 (s), 21.0 (s), 18.4 (s), 18.3 (s), 18.2 (s), 17.8 (s). UV−vis (CH_2Cl_2, λ (nm) (ε, M^{-1} cm^{-1}): 510 (3.30 × 10^3). Anal. Calcd for $C_{58}H_{58}F_7N_4P_5Ni$: C, 60.17; H, 5.05; N, 4.84. Found: C, 59.99; H, 4.98; N, 4.73.

*Synthesis of [(PP)Ni(COD)][B(C_6F_5)$_4$] (**4**).* Compound **1** (114 mg, 0.228 mmol) was dissolved in 5 mL of CH_2Cl_2, and to this light yellow solution was added K[B(C_6F_5)$_3$] (164 mg, 0.228 mmol). The mixture was allowed to stir at room temperature for 12 h. This mixture was then added to Ni(COD)$_2$ (63 mg, 0.23 mmol) and was allowed to stir for an additional 3 h. The resulting dark red mixture was filtered through Celite, and the volatiles were removed from the dark red filtrate in vacuo. The remaining residue was washed twice with 5 mL of pentane and dried under a vacuum to yield analytically pure product as a red solid. Yield: 292 mg, 98%. ^{1}H NMR (400 MHz, CD_2Cl_2): δ 7.91 (dd, 1H, $^3J_{HH}$ = 8.1 Hz, Ar-*H*), 7.54−7.43 (m, 11H, P-Ar-*H*, Ar-*H*), 7.26 (dd, 1H, $^3J_{HH}$ = 7.5 Hz, Ar-*H*), 7.18 (s, 2H, Mes-*H*), 7.12 (dd, 1H, $^3J_{HH}$ = 7.6 Hz, Ar-*H*), 5.15 (m, 2H, COD-CH), 4.33 (br, 2H, COD−C*H*), 4.04 (m, 2H, CH_2), 3.72 (m, 2H, CH_2), 2.45 (s, 6H, CH_3), 2.40 (s, 3H, CH_3), 2.01 (m, 2H, COD−CH_2), 1.73 (m, 2H, COD−CH_2), 1.68 (m, 2H, COD−CH_2), 1.16 (m, 2H, COD−CH_2). ^{31}P{^{1}H} NMR (161.8 MHz, CD_2Cl_2): δ 229.8 (s), 12.1 (s). ^{19}F{^{1}H} NMR (376 MHz, CD_2Cl_2): δ −134.0 (d, 8F), −164.6 (t, 4F), −168.4 (t, 8F). ^{13}C{^{1}H} NMR (100.5 MHz, CD_2Cl_2): δ 148.6 (bm, $^1J_{CF}$ = 238.4 Hz), 145.0 (dd, $^3J_{CP}$ = 6.7 Hz, $^2J_{CP}$ = 14.8 Hz), 140.8 (s), 138.6 (bm, $^1J_{CF}$ = 247.0 Hz), 136.7 (bm, $^1J_{CF}$ = 243.2 Hz), 136.6 (d, $^3J_{CP}$ = 2.9 Hz), 133.6 (s), 133.4 (s), 133.3 (s), 132.9 (d, $^3J_{CP}$ = 7.6 Hz), 132.5 (d, $^3J_{CP}$ = 11.4 Hz), 130.6 (s), 130.2 (s), 129.6 (d, $^3J_{CP}$ = 9.54 Hz), 125.2 (d, $^3J_{CP}$ = 4.8 Hz), 124.4 (br), 120.6 (d, $^1J_{CP}$ = 38.2 Hz), 118.9 (m), 97.9 (s), 96.6 (s), 50.7 (s), 50.2 (s), 31.3 (s), 27.2 (s), 21.2 (s), 18.3 (s). UV−vis (CH_2Cl_2, λ (nm) (ε, M^{-1} cm^{-1}): 460 (2.29 × 10^3). Anal. Calcd for $C_{61}H_{41}N_2P_2BF_{20}Ni$: C, 55.78; H, 3.15; N, 2.13. Found: C, 55.76; H, 3.21; N, 2.33.

*Synthesis of [(PP)Ni(COD)][BPh_4] (**5**).* Compound **1** (148 mg, 0.295 mmol) was dissolved in 5 mL of CH_2Cl_2, and to this light yellow solution was added $NaBPh_4$ (101 mg, 0.295 mmol). The mixture was allowed to stir at room temperature for 30 min. This mixture was then added to Ni(COD)$_2$ (81 mg, 0.30 mmol) and was allowed to stir for an additional 3 h. The resulting dark red mixture was filtered through Celite, and the volatiles were removed from the dark red filtrate in vacuo. The residue was washed twice with 5 mL of pentane and dried under a vacuum to yield analytically pure product as a red solid. Yield: 265 mg, 95%. ^{1}H NMR (400 MHz, CD_2Cl_2): δ 7.91 (dd, 1H, $^3J_{HH}$ = 7.8 Hz, Ar-*H*), 7.65 (m, 1H, Ar-*H*), 7.60−7.44 (m, 10H, P-Ar-H), 7.34 (br, 8H, B-Ar-*H*), 7.25 (dd, 1H, $^3J_{HH}$ = 7.8 Hz, Ar-*H*), 7.20 (s, 2H, Mes-*H*), 7.00 (t, 8H, $^3J_{HH}$ = 7.4 Hz, B-Ar-*H*), 6.92 (m, 1H, Ar-*H*), 6.83 (t, 4H, $^3J_{HH}$ = 7.0 Hz, B-Ar-*H*), 5.14 (m, 2H, COD-C*H*), 4.33 (br, 2H, COD-C*H*), 3.57 (m, 2H, CH_2), 3.39 (m, 2H, CH_2), 2.43 (s, 3H, CH_3), 2.39 (s, 6H, CH_3), 2.02 (m, 2H, COD-CH_2), 1.73 (m, 2H, COD-CH_2), 1.66 (m, 2H, COD-CH_2), 1.17 (m, 2H, COD−CH_2). ^{31}P{^{1}H} NMR (161.8 MHz, CD_2Cl_2): δ 229.9 (s), 11.9 (s). ^{13}C{^{1}H} NMR (100.5 MHz, CD_2Cl_2): δ 164.3 (dd, J_{CB} = 49.6 Hz, J_{CB} = 98.7 Hz), 144.8 (dd, $^3J_{CP}$ = 6.7 Hz, $^2J_{CP}$ = 14.8 Hz), 140.5 (s), 136.6 (d, $^3J_{CP}$ = 3.8 Hz), 136.2 (s), 133.4 (s), 133.3 (s), 133.2 (s), 132.9 (m), 132.4 (d, $^3J_{CP}$ = 3.8 Hz), 131.0 (s), 130.5 (s), 129.5 (d, $^3J_{CP}$ = 1.9 Hz), 125.9 (dd, $^3J_{CP}$ = 2.9 Hz, $^3J_{CP}$ = 4.8 Hz), 125.0 (d, $^3J_{CP}$ = 5.7 Hz), 122.1 (s), 120.2 (d, $^1J_{CP}$ = 37.2 Hz), 119.2 (m), 97.6 (s), 96.2 (s), 50.6 (s), 50.1 (s), 31.3 (s), 27.2 (s), 21.3 (s), 18.4 (s). UV−vis (CH_2Cl_2, λ (nm) (ε, M^{-1} cm^{-1}): 460 (1.98 × 10^3). Anal. Calcd for $C_{61}H_{61}N_2P_2BNi$: C, 76.83; H, 6.45; N, 2.94. Found: C, 76.69; H, 6.44; N, 3.04.

*Synthesis of [(PP)Ni(PMe_3)$_2$][BPh_4] (**6**).* Compound **5** (108 mg, 0.114 mmol) was dissolved in 2 mL of trifluorotoluene, and to this dark red solution was added trimethylphosphine (23.5 μL, 0.228 mmol). The reaction mixture became purple immediately. After stirring for 2 h, the resulting purple solution was concentrated to 1 mL and layered with 0.5 mL of Et_2O for 12 h, affording **6** as purple crystals suitable for X-ray crystallography. Once collected, the crystals were washed once with 5 mL of Et_2O and further dried in vacuo (106 mg, 93%). ^{1}H NMR (400 MHz, CD_2Cl_2): δ 7.51 (m, 1H, Ar-*H*), 7.48−7.45 (m, 2H, B-Ar-*H*, Ar-*H*), 7.43−7.39 (m, 4H, B-Ar-*H*), 7.31−7.29 (br m, 11H, B-Ar-*H*, P-Ar-*H*), 7.27−7.22 (m, 2H, B-Ar-*H*), 7.13 (dd, 1H, $^3J_{HH}$ = 7.4 Hz, Ar-*H*), 7.02 (m, 9H, B-Ar-*H*, Ar-*H*), 6.92 (s, 2H, Mes-*H*), 6.86 (m, 4H, B-Ar-*H*), 3.97 (br, 2H, CH_2), 3.40 (br, 2H, CH_2), 2.27 (s, 3H, Mes-CH_3), 1.92 (s, 6H, Mes-CH_3), 1.02 (d, 18H, P-CH_3). ^{31}P{^{1}H} NMR (161.8 MHz, CD_2Cl_2): δ 236.0 (dt, 1P, $^2J_{PP}$ = 58.8, 50.3 Hz), 18.8 (d, 1P, $^2J_{PP}$ = 43.3 Hz), −17.4 (d, 2P, $^2J_{PP}$ = 62.4 Hz, PMe_3). ^{13}C{^{1}H} NMR (100.5 MHz, CD_2Cl_2): δ 164.4 (dd, J_{CB} = 49.6 Hz, J_{CB} = 98.7 Hz), 145.1 (dd, $^3J_{CP}$ = 11.4 Hz), 139.3 (s), 136.3 (s), 135.3 (ddd, $^3J_{CP}$ = 5.7 Hz, $^3J_{CP}$ = 12.4 Hz, $^1J_{CP}$ = 32.4 Hz), 133.4 (d, $^2J_{CP}$ = 14.3 Hz), 133.1 (d, $^3J_{CP}$ = 11.4 Hz), 132.3 (s), 131.6 (s), 131.5 (d, $^3J_{CP}$ = 2.9 Hz), 130.7 (d, $^3J_{CP}$ = 1.9 Hz), 130.1 (s), 129.1 (d, $^3J_{CP}$ = 9.5 Hz), 125.9 (dd, $^3J_{CP}$ = 2.9 Hz, $^3J_{CP}$ = 4.8 Hz), 125.5 (m),

DOI: 10.1021/acs.inorgchem.5b01363
Inorg. Chem. 2015, 54, 8717−8726

125.4 (s), 122.1 (s), 120.6 (m), 49.7 (s), 49.5 (s), 21.3 (dm, $^1J_{CP}$ = 22.9 Hz), 21.1 (s), 18.2 (s). UV−vis (CH_2Cl_2, λ (nm) (ε, M^{-1} cm^{-1}): 500 (1.79×10^3). Anal. Calcd for $C_{59}H_{67}BN_2P_4Ni$: C, 71.04; H, 6.77; N, 2.81. Found: C, 70.95; H, 6.68; N, 3.06.

*Synthesis of [(PP)Ni(PPh$_3$)$_2$][BPh$_4$] (**7**).* A similar procedure to that described for **6** was followed, using **5** (104 mg, 0.109 mmol) and triphenylphosphine (57 mg, 0.22 mmol). The reaction mixture became purple immediately. After stirring for 2 h, the resulting purple solution was concentrated to 1 mL and layered with 0.5 mL of Et_2O for 12 h, affording **7** as purple crystals suitable for X-ray crystallography. Once collected, the crystals were washed once with 5 mL of Et_2O and further dried in vacuo. (134 mg, 90%). ^{1}H NMR (400 MHz, CD_2Cl_2): δ 7.68 (m, 1H, Ar-*H*), 7.60 (m, 2H, Ar-*H*), 7.54 (m, 1H, Ar-*H*), 7.38 (br, 10H, P-Ar-*H*), 7.25 (m, 8H, B-Ar-*H*), 7.15−7.03 (m, 12H, P-Ar-*H*), 6.95−6.84 (m, 24H, P-Ar-*H*, Mes-*H*, Ar-*H*), 6.82−6.77 (m, 8H, B-Ar-*H*), 3.79 (br, 2H, CH_2), 3.30 (br, 2H, CH_2), 2.46 (s, 3H, CH_3), 1.44 (s, 6H, CH_3). ^{31}P{^{1}H} NMR (161.8 MHz, CD_2Cl_2): δ 227.5 (dt, 1P, $^2J_{PP}$ = 67.6 Hz, $^2J_{PP}$ = 50.3 Hz), 34.0 (d, 2P, $^2J_{PP}$ = 67.6 Hz), 10.7 (d, 1P, $^2J_{PP}$ = 46.7 Hz). ^{13}C{^{1}H} NMR (100.5 MHz, CD_2Cl_2): δ 164.7 (dd, J_{CB} = 49.6 Hz, J_{CB} = 98.7 Hz), 146.8 (s), 138.9 (s), 136.6 (d, $^3J_{CP}$ = 2.9 Hz), 136.3 (s), 135.2 (br d, $^3J_{CP}$ = 2.9 Hz), 134.3 (s), 134.0 (d, $^2J_{CP}$ = 13.4 Hz), 133.9 (s), 133.7 (d, $^3J_{CP}$ = 12.4 Hz), 132.2 (d, $^3J_{CP}$ = 10.5 Hz), 130.6 (s), 130.4 (s), 130.0 (s), 129.1 (d, $^3J_{CP}$ = 2.9 Hz), 128.8 (d, $^1J_{CP}$ = 55.3 Hz), 128.5 (d, $^3J_{CP}$ = 9.5 Hz,), 127.7 (s), 126.0 (dd, $^3J_{CP}$ = 2.9 Hz, $^3J_{CP}$ = 5.7 Hz), 125.4 (m), 122.1 (s), 118.9 (m), 51.5 (s), 51.2 (s), 21.2 (s), 17.8 (s). UV−vis (CH_2Cl_2, λ(nm) (ε, $M^{-1}cm^{-1}$): 510 (2.06×10^3). Anal. Calcd for $C_{89}H_{79}BN_2P_4Ni$: C, 78.03; H, 5.81; N, 2.04. Found: C, 77.87; H, 5.93; N, 1.91.

*Synthesis of [(PP-Cl)NiCl$_2$] (**8**).* Ni(DME)Cl_2 (28 mg, 0.13 mmol) was added to a solution of compound **1** (63 mg, 0.13 mmol) in 5 mL of CH_2Cl_2. The mixture was allowed to stir at room temperature for 24 h. The orange mixture was filtered through Celite, and the volatiles were removed in vacuo. The residue was washed once with 5 mL of Et_2O and dried in vacuo to yield analytically pure product as an orange solid. Crystals suitable for X-ray crystallography were grown via layering pentane onto a concentrated DCM solution of **8**. Yield: 66 mg, 83%. ^{1}H NMR (400 MHz, CD_2Cl_2): δ 7.85 (dd, 2H, $^3J_{HH}$ = 8.4 Hz, Ar-*H*), 7.68−7.44 (m, 9H, P-Ar-*H*), 7.11 (m, 2H, P-Ar-*H*, Ar-*H*), 6.89 (br, 2H, Mes-*H*), 6.63 (dd, 1H, $^3J_{HH}$ = 9.4 Hz, Ar-*H*), 3.99 (br, 1H, CH_2), 3.51 (m, 1H, CH_2), 3.49 (m, 2H, CH_2), 2.52 (s, 3H, CH_3), 2.37 (s, 3H, CH_3), 2.26 (s, 3H, CH_3). ^{31}P{^{1}H} NMR (161.8 MHz, CD_2Cl_2): δ 106.9 (d, 1P, $^2J_{PP}$ = 121.4 Hz), 12.6 (d, 1P, $^2J_{PP}$ = 121.4 Hz). ^{13}C{^{1}H} NMR (100.5 MHz, CD_2Cl_2): δ 145.1 (d, $^3J_{CP}$ = 7.6 Hz), 138.1 (s), 137.1 (s), 136.6 (d, $^3J_{CP}$ = 5.7 Hz), 136.2 (s), 135.5 (s), 134.6 (d, $^3J_{CP}$ = 9.5 Hz), 134.3 (s), 134.1 (d, $^3J_{CP}$ = 10.5 Hz), 132.5 (d, $^3J_{CP}$ = 1.9 Hz), 131.6 (d, $^3J_{CP}$ = 2.9 Hz), 129.7 (s), 129.6 (s), 129.5 (d, $^3J_{CP}$ = 10.5 Hz), 129.2 (s), 128.7 (d, $^3J_{CP}$ = 11.5 Hz), 124.8 (m), 124.3 (s), 119.0 (m), 118.6 (dd, $^3J_{CP}$ = 10.5 Hz, $^1J_{CP}$ = 52.5 Hz), 52.5 (s), 45.1 (s), 21.1 (s), 19.6 (s), 19.0 (s). UV−vis (CH_2Cl_2, λ (nm) (ε, M^{-1} cm^{-1}): 460 (2.20×10^3). Anal. Calcd for $C_{29}H_{29}N_2P_2Cl_3Ni$: C, 55.06; H, 4.62; N, 4.43. Found: C, 55.16; H, 4.47; N, 4.55.

X-ray Crystallography Procedures. All operations were performed on a Bruker-Nonius Kappa Apex2 diffractometer, using graphite-monochromated Mo Kα radiation. All diffractometer manipulations, including data collection, integration, scaling, and absorption corrections were carried out using the Bruker Apex2 software.[15] Preliminary cell constants were obtained from three sets of 12 frames. Crystallographic parameters are provided in Tables S1 and S2 in the Supporting Information, and further experimental crystallographic details are described for each compound in the Supporting Information (pages S16−S29).

Computational Details. All calculations were performed using Gaussian 09[16] for the Linux operating system. Density functional theory calculations were carried out using the B3LYP hybrid functional.[17] A mixed-basis set was employed, using the LANL2DZ-(p,d) double ζ basis set with effective core potentials for phosphorus, chlorine, and nickel[18] and Gaussian09's internal LANL2DZ basis set (equivalent to D95V[19]) for carbon, oxygen, nitrogen, and hydrogen. Using crystallographically determined geometries as the starting point, the geometries were optimized to minimum, followed by analytical frequency calculations to confirm that no imaginary frequencies were present. Single point NBO calculations were then performed on the optimized geometries of **2**, **4**, and **6** using NBO 3.1[20] as implemented in Gaussian 09.

■ ASSOCIATED CONTENT

Ⓢ Supporting Information

The Supporting Information is available free of charge on the ACS Publications website at DOI: 10.1021/acs.inorgchem.5b01363.

^{1}H and ^{31}P NMR spectra for compounds **1**−**8** and refinement details for **1**−**3** and **6**−**8**, computational details, and additional spectral data (PDF)

Additional crystallographic data (CIF)

■ AUTHOR INFORMATION

Corresponding Author

*E-mail: thomasc@brandeis.edu.

Author Contributions

The manuscript was written through contributions of all authors. All authors have given approval to the final version of the manuscript.

Notes

The authors declare no competing financial interest.

■ ACKNOWLEDGMENTS

This material is based upon work supported by the National Science Foundation under award number CHE-1148987. The authors thank Keith Fritzsching (Brandeis University) for assistance with the TOCSY experiment. The authors are also grateful for access to the Brandeis University high performance computing cluster.

■ REFERENCES

(1) (a) Bansal, R. K.; Gudat, D. In *Phosphorus Heterocycles II*; Springer: Berlin/Heidelberg; Vol. *21*, pp 63−102. (b) Gudat, D. *Coord. Chem. Rev.* **1997**, *163*, 71−106. (c) Gudat, D. *Eur. J. Inorg. Chem.* **1998**, *1998*, 1087−1094. (d) Nakazawa, H. *J. Organomet. Chem.* **2000**, *611*, 349−363. (e) Cowley, A. H.; Kemp, R. A. *Chem. Rev.* **1985**, *85*, 367−382.

(2) (a) Pan, B.; Bezpalko, M. W.; Foxman, B. M.; Thomas, C. M. *Dalton Trans.* **2012**, *41*, 9083−9090. (b) Pan, B.; Xu, Z.; Bezpalko, M. W.; Foxman, B. M.; Thomas, C. M. *Inorg. Chem.* **2012**, *51*, 4170−4179. (c) Pan, B.; Evers-McGregor, D. A.; Bezpalko, M. W.; Foxman, B. M.; Thomas, C. M. *Inorg. Chem.* **2013**, *52*, 9583−9589. (d) Caputo, C. A.; Jennings, M. C.; Tuononen, H. M.; Jones, N. D. *Organometallics* **2009**, *28*, 990−1000. (e) Caputo, C. A.; Brazeau, A. L.; Hynes, Z.; Price, J. T.; Tuononen, H. M.; Jones, N. D. *Organometallics* **2009**, *28*, 5261−5265. (f) Price, J. T.; Lui, M.; Jones, N. D.; Ragogna, P. J. *Inorg. Chem.* **2011**, *50*, 12810−12817. (g) Förster, D.; Nickolaus, J.; Nieger, M.; Benkõ, Z.; Ehlers, A. W.; Gudat, D. *Inorg. Chem.* **2013**, *52*, 7699−7708. (h) Nickolaus, J.; Bender, J.; Nieger, M.; Gudat, D. *Eur. J. Inorg. Chem.* **2014**, *2014*, 3030−3036. (i) Hardman, N. J.; Abrams, M. B.; Pribisko, M. A.; Gilbert, T. M.; Martin, R. L.; Kubas, G. J.; Baker, R. T. *Angew. Chem., Int. Ed.* **2004**, *43*, 1955−1958. (j) Abrams, M. B.; Scott, B. L.; Baker, R. T. *Organometallics* **2000**, *19*, 4944−4956. (k) Spinney, H. A.; Yap, G. P. A.; Korobkov, I.; DiLabio, G.; Richeson, D. S. *Organometallics* **2006**, *25*, 3541−3543.

(3) (a) Pan, B.; Bezpalko, M. W.; Foxman, B. M.; Thomas, C. M. *Organometallics* **2011**, *30*, 5560−5563. (b) Burck, S.; Daniels, J.; Gans-Eichler, T.; Gudat, D.; Nättinen, K.; Nieger, M. *Z. Anorg. Allg. Chem.* **2005**, *631*, 1403−1412. (c) Hutchins, L. D.; Light, R. W.; Paine, R. T. *Inorg. Chem.* **1982**, *21*, 266−272. (d) Hutchins, L. D.; Duesler, E. N.; Paine, R. T. *Organometallics* **1982**, *1*, 1254−1256. (e) Stadelmann, B.; Bender, J.; Forster, D.; Frey, W.; Nieger, M.; Gudat, D. *Dalton Trans.*

DOI: 10.1021/acs.inorgchem.5b01363
Inorg. Chem. 2015, 54, 8717−8726

2015, *44*, 6023−6031. (f) Kawamura, K.; Nakazawa, H.; Miyoshi, K. *Organometallics* **1999**, *18*, 1517−1524. (g) Nakazawa, H.; Yamaguchi, Y.; Kawamura, K.; Miyoshi, K. *Organometallics* **1997**, *16*, 4626−4635. (h) Nakazawa, H.; Yamaguchi, Y.; Mizuta, T.; Ichimura, S.; Miyoshi, K. *Organometallics* **1995**, *14*, 4635−4643. (i) Bennett, D. W.; Parry, R. W. *J. Am. Chem. Soc.* **1979**, *101*, 755−757. (j) Montemayor, R. G.; Sauer, D. T.; Fleming, S.; Bennett, D. W.; Thomas, M. G.; Parry, R. W. *J. Am. Chem. Soc.* **1978**, *100*, 2231−2233. (k) Light, R. W.; Paine, R. T. *J. Am. Chem. Soc.* **1978**, *100*, 2230−2231.

(4) Snow, S. S.; Jiang, D. X.; Parry, R. W. *Inorg. Chem.* **1987**, *26*, 1629−1631.

(5) Hamilton, C. W.; Morris, D. E.; Blair, M. W.; Jenson, N. J.; Martin, R. L.; Cross, J. L.; Sutton, A. D.; Jantunen, K. C.; Scott, B. L.; Baker, R. T.; *INOR 50-When is addition of X-Y to M not oxidative?* The 235th ACS National Meeting, New Orleans, LA, April 6−10, 2008.

(6) Rosenberg, L. *Coord. Chem. Rev.* **2012**, *256*, 606−626.

(7) Day, G. S.; Pan, B.; Kellenberger, D. L.; Foxman, B. M.; Thomas, C. M. *Chem. Commun.* **2011**, *47*, 3634−3636.

(8) While we have only reported Pt and Pd complexes with the $[PPP]^+$ ligand thus far, preliminary results suggest very similar geometries and electronic structures are accessed with Ni(0). A manuscript describing these findings is forthcoming.

(9) Wheaton, C. A.; Bow, J.-P. J.; Stradiotto, M. *Organometallics* **2013**, *32*, 6148−6161.

(10) Yang, L.; Powell, D. R.; Houser, R. P. *Dalton Trans.* **2007**, 955−964.

(11) The PF_6^- and $[B(C_6F_5)_4]^-$ salt of the $[PP]^+$ ligand are stable in the solid state but react readily with adventitious water. Over time, the $[PP][BPh_4]$ salt decomposed via multiple pathways, leading to a mixture of at least four products identified by ^{31}P NMR spectroscopy.

(12) There are two similar independent molecules in the asymmetric unit of **7**, and the distances for the second molecule are listed in brackets.

(13) Melenkivitz, R.; Mindiola, D. J.; Hillhouse, G. L. *J. Am. Chem. Soc.* **2002**, *124*, 3846−3847.

(14) Boudier, A.; Breuil, P.-A. R.; Magna, L.; Olivier-Bourbigou, H.; Braunstein, P. *J. Organomet. Chem.* **2012**, *718*, 31−37.

(15) *Apex 2, Version 2 User Manual, M86-E01078*; Bruker Analytical X-ray Systems: Madison, WI, 2006.

(16) Frisch, M. J.; Trucks, G. W.; Schlegel, H. B.; Scuseria, G. E.; Robb, M. A.; Cheeseman, J. R.; Scalmani, G.; Braone, V.; Mennucci, B.; Petersson, G. A.; et al. *Gaussian 09*, Revision A.2; Gaussian, Inc.: Wallingford, CT, 2009 (see Supporting Information for full reference).

(17) (a) Becke, A. D. *J. Chem. Phys.* **1993**, *98*, 5648−5652. (b) Lee, C.; Yang, W.; Parr, R. G. *Phys. Rev. B: Condens. Matter Mater. Phys.* **1988**, *37*, 785−789.

(18) (a) Wadt, W. R.; Hay, P. J. *J. Chem. Phys.* **1985**, *82*, 284−298. (b) Hay, P. J.; Wadt, W. R. *J. Chem. Phys.* **1985**, *82*, 270−283. (c) Hay, P. J.; Wadt, W. R. *J. Chem. Phys.* **1985**, *82*, 299−310. (d) Roy, L. E.; Hay, P. J.; Martin, R. L. *J. Chem. Theory Comput.* **2008**, *4*, 1029−1031.

(19) Dunning, T. H. H, P. J. *In Modern Theoretical Chemistry*; Plenum: New York, 1976; Vol. 3.

(20) Glendening, E. D.; Reed, A. E.; Carpenter, J. E.; Weinhold, F. *NBO*, version 3.1.

DOI: 10.1021/acs.inorgchem.5b01363
Inorg. Chem. 2015, 54, 8717−8726